New Clues to Reveal Origins of Hot- and Warm-Jupiter: Mutual Occurrence Rate of Hot Jupiter Warm Jupiter and Cold Jupiter

Xiangning Su
Nanjing University https://orcid.org/0000-0003-3624-6881
Hui Zhang (zhangh@shao.ac.cn)
Shanghai Astronomical Observatory https://orcid.org/0000-0003-3491-6394
Jilin Zhou
Nanjing University https://orcid.org/0000-0003-1680-2940

Article

Keywords: Exoplanet, Occurrence rate, effective temperature , giant planet catalogs

Posted Date: September 22nd, 2021

DOI: https://doi.org/10.21203/rs.3.rs-877562/v1

New Clues to Reveal Origins of Hot- and Warm-Jupiter: Mutual Occurrence Rate of Hot Jupiter, Warm Jupiter and Cold Jupiter

Xiang-Ning Su[1,3], Hui Zhang[1,2,3,*], and Ji-Lin Zhou[1,3]

[1]School of Astronomy and Space Science, Nanjing University, Nanjing 210023, People's Republic of China
[2]Shanghai Astronomical Observatory, Chinese Academy of Sciences, Shanghai 200030, China
[3]Key Laboratory of Modern Astronomy and Astrophysics, Ministry of Education, Nanjing 210023, People's Republic of China
[*]zhangh@shao.ac.cn

ABSTRACT

Many works based on the correlations between the occurrence rate of various giant planets and stellar properties of their hosts have provided clues revealing planetary formation processes. However, few researches have focused on the mutual occurrence rate of different type of planets and their dependency upon the stellar properties, which may help to provide an insight into the dynamics evolution history of planetary systems. To investigate the mutual occurrence rates, first we define three types of giant planets, i.e. cold Jupiter(CJ), warm Jupiter(WJ) and hot Jupiter(HJ), according to their position normalized by the snow-line in the system, $a_p > a_{snow}$, $0.1a_{snow} < a_p \leq a_{snow}$ and $a_p \leq 0.1a_{snow}$, respectively. Then, we derive their occurrence rates(η_{HJ},η_{WJ},η_{CJ}) considering completeness correction caused by different detection methods (RV and transit) and surveys (HARPS& CORALIE and Kepler). Finally, we investigate the correlation between the mutual occurrence rates, i.e. η_{CJ}/η_{WJ} or η_{WJ}/η_{HJ}, and various stellar properties, e.g. stellar metallicity and effective temperature T_{eff}. We find that η_{WJ} from RV and transit surveys show a similar increasing trend with the increasing stellar effective temperature when $T_{eff} \leq 6100K$. While η_{CJ} from RV samples is almost flat within $T_{eff} \in (4600K, 6100K]$, and η_{HJ} from transit samples is increasing with increasing stellar effective temperature within $3600K < T_{eff} < 7100K$. Further more, we find that the mutual occurrence rate between CJ and WJ, i.e. η_{CJ}/η_{WJ}, shows a decreasing trend with the increasing stellar effective temperature. In contrary, the ratio η_{WJ}/η_{HJ} is reversely depends on the stellar effective temperature. After a series of consistency tests, our results suggest the in-situ hypothesis can be excluded from the formation process of both WJ and HJ. However, the origin and evolution history of HJ may be quite different from that of WJ.

keywords: Exoplanet, Occurrence rate, effective temperature , giant planet catalogs

Introduction

The formation of warm Jupiter(defined only by their orbital period, from 10 to 200 days) is one of most important components to build up the general framework of giant planet formation and evolution process. Because of its rarity and mystery, the formation mechanism of Warm Jupiter is still far from well understood. There are some debates on the formation mechanism of warm Jupiter, for example, whether warm Jupiter experienced various orbital migrations, or formed in situ? Some people believe the high-eccentricity migration could not explain the formation of warm Jupiter born beyond 1 AU[1]. And disk migration may also explain the high eccentricity of some warm Jupiters[2]. However, there are also some evidence showing that warm Jupiter may form in situ[3]. In contrast, due to lower observation requirements, much more hot Jupiters have been found which enable us to investigate their formation process thorough statistics ways. Although some people put forward the hot Jupiters might form in situ[4–6], most people believed that hot Jupiters should form through some kind of migration scenarios: one theory is the disk migration,i.e., giant planet migrate into close-in orbit through the gaseous disk[7–9] , the other one is the high-eccentricity migration, where a giant planet is excited to a high-eccentricity orbit by mechanisms like Lidov Kozai effect[10,11] and further delivered to the close-in orbit by the tidal dissipation[12–15]. Based on disk migration theory, hot Jupiters, at least some of them, are believed to be results of inward migrated warm Jupiters[16]. However, according to the high companion fraction of warm Jupiters[3,17], there suppose to be some differences in the formation or dynamical history of warm Jupiters and hot Jupiters.

Most of previous studies have focused on the occurrence rate of a particular kind of planets and its dependence versus other planetary or stellar properties, e.g. occurrence rate of planets have an increases trend with decreasing planet radius and increasing orbital period[18], for Earth-size to Neptune-size planets (1–4 $R_\oplus$, Kepler planets), the occurrence rate of planets

is successively higher toward later spectral types at all orbital periods[19]. Even though occurrence rate of Kepler planets be found rises only weakly with metallicity of their host stars, but for giant planets, they tend to form around more metal-rich stars[20]. Furthermore, the occurrence rate of giant planets with positive correlation to the mass of host stars[18]. Some previous statistical studies have found giant planets show a rising occurrence rate with orbital semi-major axis out to 1 AU[21,22], similarly, recent studies suggest that the occurrence rate of giant planets increasing at longer periods but appear to fall off after 100 day[23]. Besides, the number of planets decreases towards higher stellar effective temperature and stellar mass[24]. Because limited observation baseline, only K type stars harbor giant planet outside the snowline (corresponding to the equilibrium temperature of planets is 170K[25]) in Kepler sample. Nevertheless, the radial velocity(RV) survey found many exoplanets with mass greater than Neptune mass well beyond 1AU[26–28]. Based on RV-detected planets, some people found an increasing occurrence rate of planets with decreasing planetary mass for planets between $3M_{\oplus}$ to $1000M_{\oplus}$[26]. The occurrence rate of giant planets also show a rising tend with the longer orbital period, and the occurrence rate of planet beyond $1AU$ is several times higher than that of close giant planets[29]. There are also some analysis characterizing the relationship between the occurrence rate of these planets and properties of their host stars based the RV survey. Occurrence rate of giant planet correlates with both stellar metallicity[30,31] and stellar mass(for which effective temperature T_{eff} is a proxy), for example, the occurrence rate of giant planets increases towards higher metallicity of host stars[30,32,33].

All of results mentioned above are usually based on the present value of planetary orbital properties whose original distribution and dependency may have been reshaped substantially during the dynamics evolution history. The most straight forward way to solve this problem may be taking into account the stellar age of those planet hosts. For example, statistics studies focusing on the planetary occurrence rates versus stellar age could help to demonstrate the evolution traces of planetary properties directly[34]. However, due to the difficulties on obtaining accurate stellar ages of a large sample of stars with planets, the valid sample size is still quite limited for a detailed statistics study[35]. In contrast to the direct way, studies on ratio of occurrence rates of different planet populations may offer us some indirect clues on their evolution history and initial formation rates. For example, let us consider a large sample of young star systems with the initial disk properties coupled strongly to the host properties, e.g. the disk mass closely dependent on the stellar mass[36,37] and etc. Most giant planets formed outside the snowline[38](CJ) and we assume that some of them may migrate inward to become warm Jupiter (WJ) and even hot Jupiter (HJ). Then, how much ratio of CJ could have been evolved to WJ or how much ratio of WJ could have been turned into HJ, should be governed by the migration efficiency of the disk, which is therefore supposed to be highly correlated to the stellar properties, like stellar mass, effective temperature and/or stellar metallicity. That means the ratio of occurrence rates of CJ and WJs and the ratio of occurrence rates of WJ and HJ, should show a dependence on one or several stellar properties. If giant planets do not migrate at all, i.e. they form just in-situ formation, the ratio of occurrence rates would just represent the relative probability on where a giant planet may emerge, e.g. inside or beyond the snowline. Such ratio may also show a dependence on the stellar property. But it should be quite different from the results of the orbital migration models. Therefore, this stellar property dependent ratio of occurrence rates may be used to distinguish different formation and evolution mechanisms of different populations of giant planets, i.e. forming through disk migration or just in-situ.

In this work, we present our studies on the dependency between the occurrence rates of three giant planet populations and stellar properties, e.g. the effective temperature T_{eff}, of their hosts. We first divide giant planets into three populations, i.e. HJ, WJ and CJ, according to their snowline-normalized planet-host distances. Then, we assume HJ and WJ origin from WJ and CJ, respectively. And we use the ratio of occurrence rate of WJ(CJ) and HJ(WJ) (η_{CJ}/η_{WJ} and η_{WJ}/η_{HJ})to denote the efficiency of the transition from WJ(CJ) to HJ(WJ). Our results show that the ratio of occurrence η_{CJ}/η_{WJ} is lower when the host's T_{eff} is higher. While, in contrary, the occurrence ratio η_{WJ}/η_{HJ} is increasing when the stellar T_{eff} is also increasing. This significant different dependencies indicates that the formation and evolution mechanisms of HJ and WJ may be quite different. Our further analysis show that the decreasing T_{eff}-dependency of the occurrence ratio η_{CJ}/η_{WJ} is NOT consistent with the in-situ formation. These clues imply that some CJ migrate inward before the gaseous disk has depleted and form WJ. While, HJ are NOT those fast migrating WJ and they should form in a way that is quite different from disk migration. Major results are presented in the next section and we discuss and conclude our results.

Results and Discussion

WJ and CJ from RV samples

We use a homogeneous RV-detected giant planets sample from two RV surveys: HARPS & CORALIE, section **Methods** have illustrated RV samples in detail. To calculate the occurrence rate of both WJ and CJ around 1191 main sequence K-, G-, and F-type dwarf stars in HARPS & CORALIE surveys. And we further investigate the correlation between the ratio of this two occurrence rates and the stellar effective temperature of these giant planet hosts. To obtain the real number of giant planets that should exist within each T_{eff} bin, we carry out a detection efficiency correction. For each detected giant planet, we calculate how many other planets were missed by considering the observational bias of detection methods and survey completeness. The missing number is added into each T_{eff} bin when we calculate the occurrence rates of different giant planet samples. Note

that, due to the totally different bias in methods and survey completeness, planets found by RV and Transit surveys are treated separately(a detailed description of the method in **Methods**).

As shown in Figure 1(A), the real RV-detected numbers of WJ and CJ show a similar increasing trend when their host's stellar effective temperature T_{eff} is also increasing in the range of $4600-6100K$. When T_{eff} goes above $6100K$, the RV-detected numbers of WJ and CJ both drop downward sharply. From the view of occurrence rate, there is also a drop of η_{WJ} in the $6100-6600K$ bin. But it doesn't change the increasing trend with stellar effective temperature in general. However, η_{CJ} is almost flat within in the T_{eff} range of $4600-6100K$. But it drops significantly in the rightmost bin where $T_{eff} \in (6100K, 6600K]$. Both the drops of WJ and CJ samples in this bin may be real reflections of deficit of giant planets around early type stars, which is also seen in our transit-detected samples(shown in Figure 1(C)). But their amplitudes and uncertainties are relatively larger and they are probably caused by the lack of high T_{eff} survey targets. Usually, early type stars whose effective temperature is higher are relatively more active and are harder to get high precision radial velocity measurements. As a result, only those quiet early type stars are selected in a RV planet survey, which leads to a smaller sample size of high T_{eff} stellar targets and additional selection bias which is not considered in the detection efficiency correction part.

To mitigate such statistic effects arose by the sample size, we further investigate the ratio of occurrence rate of CJs and WJs samples η_{CJ}/η_{WJ}. As shown in Figure 1(B), we found a monotonous decreasing trend of the ratio when the stellar effective temperature is increasing. This result shows that the frequency of CJ is relatively higher than that of WJ around cooler stars. If giant planets form outside the snowline (as CJ in our definition) and migrate inward to became WJ, then this T_{eff} dependent trend offers an indirect evidence to this process—higher stellar effective temperature means a higher disk mass in the proto-stellar disk and therefor a higher efficiency in moving giant planets inward.

HJ and WJ from Kepler samples

According to our classifications mentioned in **Methods**, only a handful giant planets released by the Kepler DR25 locate further beyond the snow line in their system, while most samples are closer and warmer and belong to the HJ or WJ sample. Similar to the RV samples, we calculate the individual occurrence rate of the HJ and WJ sample first. And then we further investigate the correlation between their ratio and the stellar effective temperature.

The planet numbers corrected by the survey completeness are shown in each stellar effective temperature bin by the histogram in Figure 1(C). The numbers of the valid survey stars which are used to derive the occurrence rate are listed in **Methods**(table 2). η_{WJ} and η_{HJ} show similar increasing trend with the increasing host effective temperature in the range of $3600K-6100K$. In the rightmost bin where $T_{eff} \in (6100K, 7100K]$, the occurrence rate keeps growing for HJ but it drops sharply for WJ. It seems that an M/K/G type star has a higher probability to host WJ than to host HJ. But for F type or hotter stars the probability reverses. The drop of WJ in the high T_{eff} bin is similar to that observed in the RV samples, however it is unlikely to be caused by the lack of long period giant planets. The vertical bars show that we have hundreds of samples for both HJ and WJ types (after survey completeness correction) within this bin.

In Figure 1(D), we show the ratio of the two occurrence rates η_{WJ}/η_{HJ}. The result also shows a value well above 1 and keeps increasing with higher stellar effective temperature when $3600K < T_{eff} < 6100K$ and drops down below 1 when $T_{eff} > 6100K$. If HJ are formed by WJ via disk migration process and higher T_{eff} means a more massive disk, then the transform from WJ to HJ should be more efficient around hotter stars and produce an inverse dependence of the η_{WJ}/η_{HJ} and the host T_{eff}. Our statistic result implies that, unlike the formation of WJ, the disk migration mechanism may not dominate the formation of HJ.

Implication to the formation of HJ and WJ

The formation of giant planets locating inside the snow line, e.g. HJ and WJ, is usually considered as an outside-in process (at least for HJ and a part of short-period WJ), i.e. giant planets form outside the snow line where the high density of solid disk leads to relatively short growth timescale of planetary embryo, and then they migration inward to become WJ or even HJ. There are two major mechanisms to explain the inward delivering of giant planets, i.e. migration through a disk which is composed of gas, dust or/and planetesimals or migration due to planet-planet scattering which is also called the high-e migration.

One of the major goals of the recent researches is to find out the major evolution track of giant planets, and distinguish to the dominated one from this two mechanisms. In this work, we study the ratio of occurrence rates of two kinds of giant planets, i.e. η_{CJ}/η_{WJ} and η_{WJ}/η_{HJ}. And we believe this outer-to-inner occurrence rate ratio and its dependence on the stellar effective temperature could help to reveal some clues on the migration efficiency when a CJ transfers to a WJ and/or a WJ becomes a HJ, where the host star is of different stellar types.

Our results have shown that the effective temperature dependence is total different for η_{CJ}/η_{WJ} and η_{WJ}/η_{HJ}, which implies the formation mechanisms of WJ and HJ are quite different as well. It seems the result on WJ could be explained by the disk-migration mechanism, while the result on HJ is contrary with the prediction from the same mechanism. There are several major possibilities need to be explored and clarified before we could jump to the final conclusion, e.g. the stellar metallicity influences, the in-situ formation mechanism and so on.

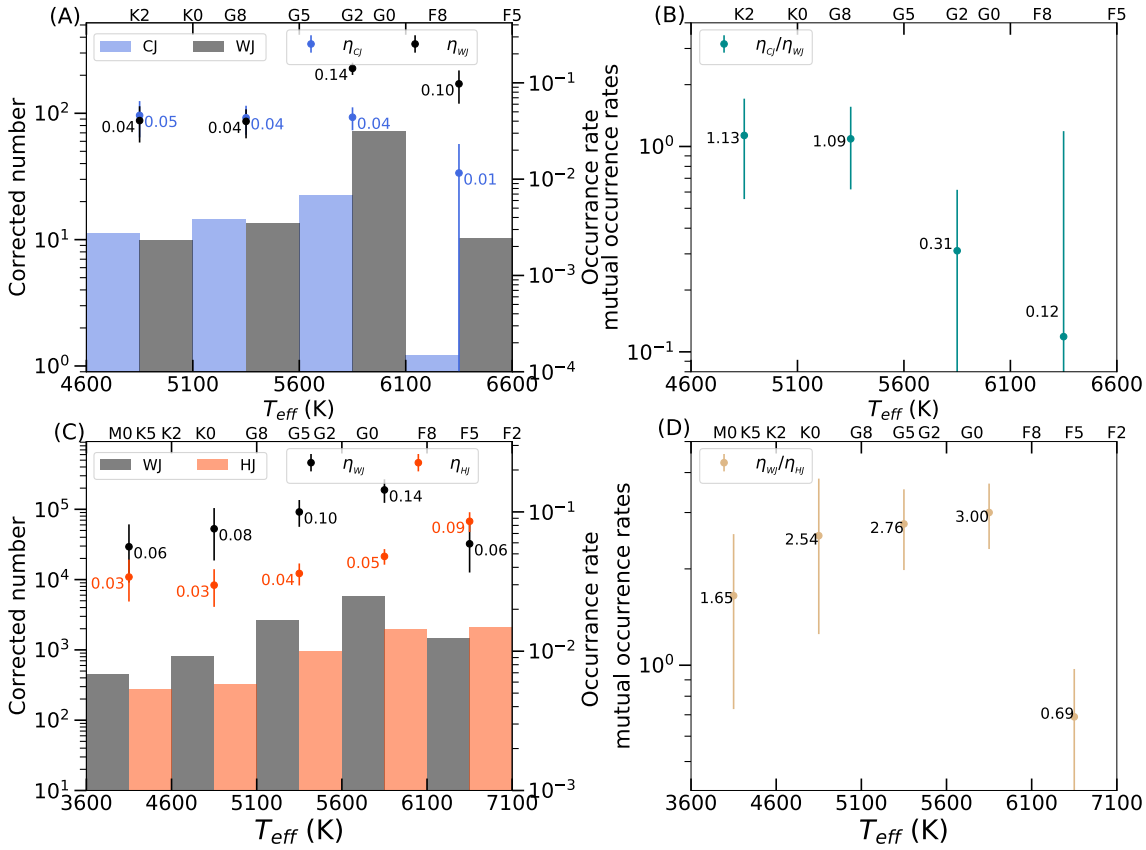

Figure 1. Corrected number, occurrence rate and mutual occurrence rate of different giant planet populations(HJ, WJ, CJ) in RV and transit survey. (A): Histogram of corrected number of giant planets(WJ(gray bar) and CJ(blue bar) detected by RV) and the occurrence rate of giant planets in four T_{eff} bins ($T_{eff} \in [4600K, 6600K]$). Where the left coordinate corresponding to corrected number, and the right coordinate corresponding to the occurrence rate.(B): the mutual occurrence rate of CJ and WJ (shown in green) in four T_{eff} bins. WJ(gray) and CJ(blue) are depicted separately. (C): Histogram of real number of giant planets(WJ(gray bar) and HJ(orange bar) detected by transit) and the occurrence rate of giant planets in five T_{eff} bins($T_{eff} \in [3600K, 7100K]$). The coordinate are same as (A).(D): the mutual occurrence rate of WJ and HJ(shown as earthy yellow) in five T_{eff} bins. WJ(gray) and HJ(orange) are depicted separately.

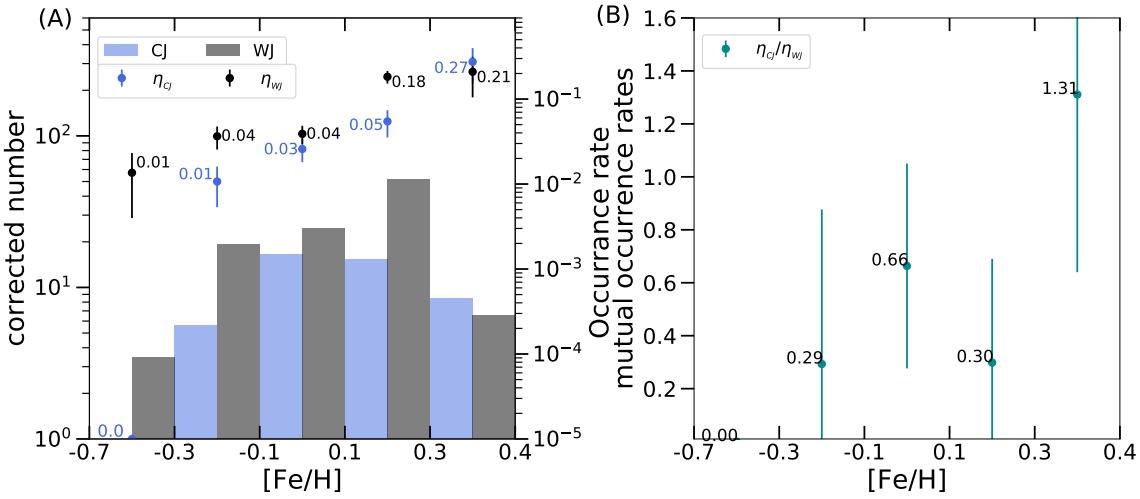

Figure 2. The occurrence-rate- stellar metallicity dependence of CJ and WJ, and the ratio of occurrence rate of CJ and WJ. (a): Histogram of corrected number of giant planets(WJ(gray bar) and CJ(blue bar)) and the occurrence rate of giant planets in five stellar metallicity bins.Where the left coordinate corresponding to corrected number, and the right coordinate corresponding to the occurrence rate. (b): the mutual occurrence rate of CJ and WJ(shown in green) in five stellar metallicity ranges. WJ(gray) and CJ(blue) are depicted separately.

The correlation between the occurrence rate of giant planets and the metallicity of their host star, has drawn a lot of attention and is treated as a critical clue to reveal how the formation process of giant planet affected by the stellar properties of its host star[19,30,33]. It is usually believed that giant planets, especially for those long period ones, e.g. WJ and CJ, are more likely to form around metal-rich stars[30,32]. To perform a sanity check and verify the consistency of our model, we also explore the stellar-metallicity dependence of warm Jupiters and cold Jupiters. The definition and samples of WJ and CJ and the method to derive their occurrence rates are all the same as our previous case. The only difference is we replace the stellar effective temperature with the stellar metallicity this time. As shown in Figure 2, for both WJ and CJ, the occurrence rate increases with an increasing metallicity of their host, which is quite consistent with previous studies. Further more, the η_{CJ}/η_{WJ} also shows an increasing trend with the increasing metallicity in general.

As we mentioned before, giants planet are believed to form slightly outside the snow-line where the solid density jumps high. They are supposed to begin with solid cores. Before the planetary core has accreted enough solid mass to trigger the effective gas accretion process, it usually suffers fast inward orbital decay due to the tidal torques exerted on it by the gaseous disk. It is usually called the type-I migration which may cause a significant orbit change within $10^4 - 10^5$ year for a planet core around several $M_\oplus$. Many planetary cores are probably delivered to a warm or even hot place from the cold region outside the snow line by this mechanism. As soon as the planet core grows above a critical mass, which is around $\sim 10M_\oplus$ depending on the disk opacity mostly, it steps into a quasi-static accretion process, after several million years, the total mass of planet above $\sim 20M_\oplus$, it steps into runaway gas accretion scenario[38] and grows up to a massive giant planet in a very short time scale, $\sim 10^3 - 10^4$ years. Then the massive planet will open a deep gap in the disk along its orbit region and its migration speed will drop down significantly to match the viscous evolution time scale of the disk, i.e. the type-II migration. While, the high metallicity of the proto-stellar disk may help to fasten the growth of the solid planet core through the pebble accretion mechanism and shorten, even avoid its fast migration era.

If we assume the metallicity of the proto-stellar disk is directly proportional to the metallicity of the host star, giant planets may grow faster around a metal-rich star and stay closer to the origin place where they form, e.g. beyond the snow line. In other words, the transferring efficiency from a CJ to a WJ will be lower around a star with higher metallicity. And the mutual occurrence rate of CJ and WJ, η_{CJ}/η_{WJ}, should increase as the stellar metallicity increases, which is just consistent with our result (see Figure 2 (b)).

All previous discussions are based on an assumption that a giant planet origins beyond the snow line and may migrate inward as it is growing up and ends up as a warm or hot Jupiter. What will happen, if the cold, warm or even hot giant planet form in-situ? Some comparisons show that our result can not explained by the in-situ mechanism (in **Methods**) and implies that WJ may have undergone some kinds of migration during its formation history.

Conclusion

In this paper, based on RV (HARPS & CORALIE) and transit (kepler) samples, we define three giant planet populations according to the normalized planetary semi-major axis (HJ:$a_p \leq 0.1a_{snow}$, WJ: $0.1a_{snow} < a_p \leq a_{snow}$, CJ: $a_p > a_{snow}$) and derive their occurrence rates. We further investigate the correlation between the mutual occurrence rate (η_{CJ}/η_{WJ} and η_{WJ}/η_{HJ}) and stellar effective temperature.

Firstly, We find that the occurrence rate of WJs is increasing first and drop downward sharply in hottest T_{eff} bin(RV: $6100-6600K$; transit: $6100-7100K$) with the increasing stellar T_{eff} both RV- and transit- detected samples. The occurrence rate of RV-detected CJ shows almost flat within in range of $4600-6100K$ then drop sharply in $6100-6600K$ bin. And the occurrence rate of transit-detected HJ is almost increasing with the increasing stellar T_{eff}.

Second, analysis results shows that there is obvious dependency between the ratio of occurrence rate of CJ and WJ and stellar T_{eff}, the ratio show a declining tendency with the increasing T_{eff}. That may means that with the increase of stellar mass, and the disk mass also become higher, the dynamical evolution efficiency of CJ are improved. Besides, from Kepler transit samples, the ratio of occurrence rate of WJ and HJ show a rising trend with increasing effective temperature of their host stars, this trend is contrary to the trend of the ratio of CJ and WJ. So, the formation and evolution process of WJ and HJ should be governed by very different mechanisms, e.g. disk migration and high-e migration, respectively.

Then, we also explore the dependency between the occurrence rates of three period defined giant planet populations and T_{eff} of hosts. The ratio of occurrence rate of WJ and HJ also show a rising trend with increasing T_{eff} of hosts. But due to the small sample of period-defined WJ, the ratio η_{CJ}/η_{WJ} don't show same trend compare with the ratio in snowline-defined sample.

Finally, according to the stellar metallicity dependence ratio of occurrence rate of CJ and WJ, we find the trend of the ratio of occurrence rate of CJ and WJ with increasing stellar metallicity is different to the trend demonstrate with T_{eff} of host stars. Then we also rule out the in-situ formation of WJ by comparing the ratio of occurrence rates, η_{CJ}/η_{WJ} to the ratio of formation rates, $\eta^{'}{}_{CJ}/\eta^{'}{}_{WJ}$ (position-independent)and $\eta^{*}{}_{CJ}/\eta^{*}{}_{WJ}$(position-dependent).

In summary, our study emphasizes the importance taking into account physical property when dividing different giant planets populations. And exploring for the ratio of occurrence rate of different planets populations may be provide a new way to study formation and evolution of planets. The results of this paper suggest that the main formation mechanism of WJ is disk migration, and it is differ from the formation mechanism of HJ.

References

1. Antonini, F., Hamers, A. S. & Lithwick, Y. Dynamical Constraints on the Origin of Hot and Warm Jupiters with Close Friends. **152**, 174, DOI: 10.3847/0004-6256/152/6/174 (2016). 1604.01781.

2. Debras, F., Baruteau, C. & Donati, J.-F. Revisiting migration in a disc cavity to explain the high eccentricities of warm Jupiters. **500**, 1621–1632, DOI: 10.1093/mnras/staa3397 (2021). 2010.14425.

3. Huang, C., Wu, Y. & Triaud, A. H. M. J. Warm Jupiters Are Less Lonely than Hot Jupiters: Close Neighbors. **825**, 98, DOI: 10.3847/0004-637X/825/2/98 (2016). 1601.05095.

4. Batygin, K., Bodenheimer, P. H. & Laughlin, G. P. In Situ Formation and Dynamical Evolution of Hot Jupiter Systems. **829**, 114, DOI: 10.3847/0004-637X/829/2/114 (2016). 1511.09157.

5. Boley, A. C., Granados Contreras, A. P. & Gladman, B. The In Situ Formation of Giant Planets at Short Orbital Periods. **817**, L17, DOI: 10.3847/2041-8205/817/2/L17 (2016). 1510.04276.

6. Bailey, E. & Batygin, K. The Hot Jupiter Period-Mass Distribution as a Signature of in situ Formation. **866**, L2, DOI: 10.3847/2041-8213/aade90 (2018). 1809.05517.

7. Goldreich, P. & Tremaine, S. Disk-satellite interactions. **241**, 425–441, DOI: 10.1086/158356 (1980).

8. Lin, D. N. C. & Papaloizou, J. On the Tidal Interaction between Protoplanets and the Protoplanetary Disk. III. Orbital Migration of Protoplanets. **309**, 846, DOI: 10.1086/164653 (1986).

9. Lin, D. N. C., Bodenheimer, P. & Richardson, D. C. Orbital migration of the planetary companion of 51 Pegasi to its present location. **380**, 606–607, DOI: 10.1038/380606a0 (1996).

10. Kozai, Y. Secular perturbations of asteroids with high inclination and eccentricity. **67**, 591–598, DOI: 10.1086/108790 (1962).

11. Lidov, M. L. The evolution of orbits of artificial satellites of planets under the action of gravitational perturbations of external bodies. **9**, 719–759, DOI: 10.1016/0032-0633(62)90129-0 (1962).

12. Rasio, F. A. & Ford, E. B. Dynamical instabilities and the formation of extrasolar planetary systems. *Science* **274**, 954–956, DOI: 10.1126/science.274.5289.954 (1996).

13. Weidenschilling, S. J. & Marzari, F. Gravitational scattering as a possible origin for giant planets at small stellar distances. **384**, 619–621, DOI: 10.1038/384619a0 (1996).

14. Ford, E. B. & Rasio, F. A. Origins of Eccentric Extrasolar Planets: Testing the Planet-Planet Scattering Model. **686**, 621–636, DOI: 10.1086/590926 (2008). astro-ph/0703163.

15. Chatterjee, S., Ford, E. B., Matsumura, S. & Rasio, F. A. Dynamical Outcomes of Planet-Planet Scattering. **686**, 580–602, DOI: 10.1086/590227 (2008). astro-ph/0703166.

16. Hallatt, T. & Lee, E. J. Can Large-scale Migration Explain the Giant Planet Occurrence Rate? **904**, 134, DOI: 10.3847/1538-4357/abc1d7 (2020). 2010.07949.

17. Steffen, J. H. *et al.* Kepler constraints on planets near hot Jupiters. *Proc. Natl. Acad. Sci.* **109**, 7982–7987, DOI: 10.1073/pnas.1120970109 (2012). 1205.2309.

18. Howard, A. W. *et al.* Planet Occurrence within 0.25 AU of Solar-type Stars from Kepler. **201**, 15, DOI: 10.1088/0067-0049/201/2/15 (2012). 1103.2541.

19. Mulders, G. D., Pascucci, I. & Apai, D. A Stellar-mass-dependent Drop in Planet Occurrence Rates. **798**, 112, DOI: 10.1088/0004-637X/798/2/112 (2015). 1406.7356.

20. Kutra, T. & Wu, Y. Kepler Planets and Metallicity. *arXiv e-prints* arXiv:2003.08431 (2020). 2003.08431.

21. Dong, S. & Zhu, Z. Fast Rise of "Neptune-size" Planets (4-8 $R_\oplus$) from P ~10 to ~250 Days—Statistics of Kepler Planet Candidates up to ~0.75 AU. **778**, 53, DOI: 10.1088/0004-637X/778/1/53 (2013). 1212.4853.

22. Santerne, A. *et al.* SOPHIE velocimetry of Kepler transit candidates. XVII. The physical properties of giant exoplanets within 400 days of period. **587**, A64, DOI: 10.1051/0004-6361/201527329 (2016). 1511.00643.

23. Fernandes, R. B., Mulders, G. D., Pascucci, I., Mordasini, C. & Emsenhuber, A. Hints for a Turnover at the Snow Line in the Giant Planet Occurrence Rate. **874**, 81, DOI: 10.3847/1538-4357/ab0300 (2019). 1812.05569.

24. Yang, J.-Y., Xie, J.-W. & Zhou, J.-L. Occurrence and Architecture of Kepler Planetary Systems as Functions of Stellar Mass and Effective Temperature. **159**, 164, DOI: 10.3847/1538-3881/ab7373 (2020). 2002.02840.

25. Hayashi, C. Structure of the Solar Nebula, Growth and Decay of Magnetic Fields and Effects of Magnetic and Turbulent Viscosities on the Nebula. *Prog. Theor. Phys. Suppl.* **70**, 35–53, DOI: 10.1143/PTPS.70.35 (1981).

26. Howard, A. W. *et al.* The Occurrence and Mass Distribution of Close-in Super-Earths, Neptunes, and Jupiters. *Science* **330**, 653, DOI: 10.1126/science.1194854 (2010). 1011.0143.

27. Mayor, M. *et al.* The HARPS search for southern extra-solar planets XXXIV. Occurrence, mass distribution and orbital properties of super-Earths and Neptune-mass planets. *arXiv e-prints* arXiv:1109.2497 (2011). 1109.2497.

28. Wittenmyer, R. A. *et al.* The Anglo-Australian Planet Search XXIV: The Frequency of Jupiter Analogs. **819**, 28, DOI: 10.3847/0004-637X/819/1/28 (2016). 1601.05465.

29. Wittenmyer, R. A. *et al.* Cool Jupiters greatly outnumber their toasty siblings: occurrence rates from the Anglo-Australian Planet Search. **492**, 377–383, DOI: 10.1093/mnras/stz3436 (2020). 1912.01821.

30. Johnson, J. A. *et al.* Retired A Stars and Their Companions. IV. Seven Jovian Exoplanets from Keck Observatory. **122**, 701, DOI: 10.1086/653809 (2010). 1003.3445.

31. Fischer, D. A. & Valenti, J. The Planet-Metallicity Correlation. **622**, 1102–1117, DOI: 10.1086/428383 (2005).

32. Neves, V. *et al.* Metallicity of M dwarfs. III. Planet-metallicity and planet-stellar mass correlations of the HARPS GTO M dwarf sample. **551**, A36, DOI: 10.1051/0004-6361/201220574 (2013). 1212.3372.

33. Mortier, A. *et al.* On the functional form of the metallicity-giant planet correlation. **551**, A112, DOI: 10.1051/0004-6361/201220707 (2013). 1302.1851.

34. Berger, T. A., Huber, D., Gaidos, E., van Saders, J. L. & Weiss, L. M. The Gaia-Kepler Stellar Properties Catalog. II. Planet Radius Demographics as a Function of Stellar Mass and Age. *arXiv e-prints* arXiv:2005.14671 (2020). 2005.14671.

35. Lu, Y. L., Angus, R., Curtis, J. L., David, T. J. & Kiman, R. Gyro-kinematic Ages for around 30,000 Kepler Stars. **161**, 189, DOI: 10.3847/1538-3881/abe4d6 (2021).

36. Pascucci, I. *et al.* A Steeper than Linear Disk Mass-Stellar Mass Scaling Relation. **831**, 125, DOI: 10.3847/0004-637X/831/2/125 (2016). 1608.03621.

37. Mulders, G. D., Pascucci, I., Ciesla, F. J. & Fernandes, R. B. The Mass Budgets and Spatial Scales of Exoplanets and Protoplanetary Disks. In *American Astronomical Society Meeting Abstracts*, vol. 53 of *American Astronomical Society Meeting Abstracts*, 317.02 (2021).

38. Pollack, J. B. *et al.* Formation of the Giant Planets by Concurrent Accretion of Solids and Gas. **124**, 62–85, DOI: 10.1006/icar.1996.0190 (1996).

39. Mathur, S. *et al.* VizieR Online Data Catalog: Revised stellar properties of Q1-17 Kepler targets (Mathur+, 2017). *VizieR Online Data Catalog* J/ApJS/229/30 (2017).

40. Thompson, S. E. *et al.* Planetary Candidates Observed by Kepler. VIII. A Fully Automated Catalog with Measured Completeness and Reliability Based on Data Release 25. **235**, 38, DOI: 10.3847/1538-4365/aab4f9 (2018). 1710.06758.

41. Brown, T. M., Latham, D. W., Everett, M. E. & Esquerdo, G. A. Kepler Input Catalog: Photometric Calibration and Stellar Classification. **142**, 112, DOI: 10.1088/0004-6256/142/4/112 (2011). 1102.0342.

42. Kepler Mission Team. VizieR Online Data Catalog: Kepler Input Catalog (Kepler Mission Team, 2009). *VizieR Online Data Catalog* V/133 (2009).

43. Berger, T. A., Huber, D., Gaidos, E. & van Saders, J. L. Revised Radii of Kepler Stars and Planets Using Gaia Data Release 2. **866**, 99, DOI: 10.3847/1538-4357/aada83 (2018). 1805.00231.

44. Mulders, G. D., Pascucci, I., Apai, D. & Ciesla, F. J. The Exoplanet Population Observation Simulator. I. The Inner Edges of Planetary Systems. **156**, 24, DOI: 10.3847/1538-3881/aac5ea (2018). 1805.08211.

45. Gaia Collaboration *et al.* Gaia Data Release 2. Summary of the contents and survey properties. **616**, A1, DOI: 10.1051/0004-6361/201833051 (2018). 1804.09365.

46. Petigura, E. A. *et al.* The California-Kepler Survey. I. High-resolution Spectroscopy of 1305 Stars Hosting Kepler Transiting Planets. **154**, 107, DOI: 10.3847/1538-3881/aa80de (2017). 1703.10400.

47. Ida, S. & Lin, D. N. C. Toward a Deterministic Model of Planetary Formation. II. The Formation and Retention of Gas Giant Planets around Stars with a Range of Metallicities. **616**, 567–572, DOI: 10.1086/424830 (2004). astro-ph/0408019.

Acknowledgements

This work is supported by the support by the National Natural Science Foundation of China (NSFC; grant No. 12073010, 11673011, 11933001).

Methods

Transit Samples and The Definitions of HJ, WJ, CJ

To build sufficient giant planets samples, we use transit-detected planets. And the Kepler DR25 offers a homogeneous sample of short- and moderate-period planets with survey completeness well determined[39,40]. We start to build our samples from the Kepler Input Catelog (KIC)[41,42](`https://exoplanetarchive.ipac.caltech.edu/cgi-bin/TblView/nph-tblView?app=ExoTbls&config=koi`) which contains 186301 stars and 8054 planetary candidates found in the Q1-Q17 data. We adopt the stellar properties after across match with Gaia Data Release 2[34], e.g. the effective temperatureT_{eff}, stellar radius $R_\star$. With these well determined properties, all the giant stars whose surface gravity $logG < 4.0$ are filtered out. And we further remove giant stars and binaries using the index of evolution state and number of companion obtained by previous study[43]. The whole stellar sample for further statistic study contains 111388 stars with T_{eff} between 3600K and 7100K.

For transiting giant planet sample we set several filters:

1. All known false positives are removed.
2. Radius of planet is updated according to previous mentioned stellar parameters. Only those giant planets with R_p between $4R_\oplus$ and $20R_\oplus$ are selected.

After use those cut, we get a homogeneous sample of transit-detected giant planet, i.e. Kepler giant planets. The sample classification of Kepler giant planets is as follows.

we usually call giant planets with orbit period less than a few days, e. g. < 10 days, hot Jupiter. However, such a definition does not have too much physics meaning. Planets with the same orbit period around different type of host stars are sometimes significantly different in their physics and dynamics properties. In this work, we adopt a definition related to the normalized orbit semi-major axis(a_p/a_{snow}) to include the stellar properties of their hosts. The normalization factor is the distance of the

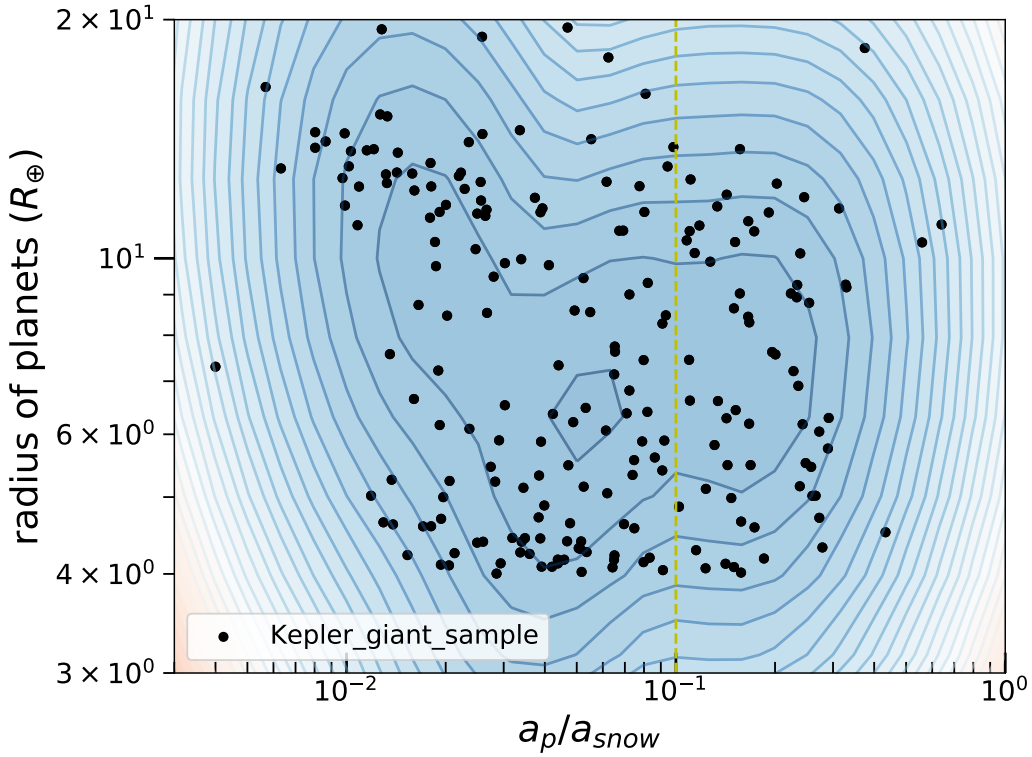

Figure 3. Normalized semi-major axis .vs. radius of planets(R_p) distribution of giant planets detected by Kepler surveys, there are a boundary(yellow dotted line) at $a_p/a_{snow} = 0.1$.

snow line a_{snow} where the equilibrium temperature $T_{eq} = 170K$ in the planetary system. The equilibrium temperature of planet is given by[25]:

$$T_p = 280(\frac{a_p}{1AU})^{-1/2}(\frac{L_\star}{L_\odot})^{1/4}K \tag{1}$$

where $L_\star$ and $L_\odot$ are the luminosity of host star and sun, due to the lower uncertainty of T_{eff} and $L_\star$ is given as

$$L_\star = 4\pi {R_\star}^2 \sigma T_{eff}^4 \tag{2}$$

where $R_\star$ is stellar radius,σ is Stefan-Boltzmann constant ,and T_{eff} is effective temperature of star. As shown in Figure 3, there are the normalized orbit semi-major axis(a_p/a_{snow}) and radius(R_p) diagram of all Kepler giant planets filtered through the process mentioned above. Based on Bayesian Information Criterion(BIC), we derive the optimal fitting model of Gaussian mixture model(GMM) for the snow line normalized semi-major axis and radius distribution. As we can see in Figure 3, there are might a boundary at $0.1a_{snow}$. So in this work, our samples were divided into 3 groups: boundaries of HJ and WJ is $0.1a_{snow}$, and a_{snow} as the boundaries of WC and CJ.

Because our Kepler giant planets have not long period giant planets with orbital semi-major axis larger than $1a_{snow}$ (avoid large uncertainty in the survey completeness calculation), so we just build HJ and WJ samples in Kepler giant planets sample. So, for a transiting giant planet(Kepler samples) , we calculate the position of snow line, a_{snow} , within its system. When its semi-major axis a_p is smaller than $0.1a_{snow}$, it belongs to the HJ sample. In contrast, when it locates further than $0.1a_{snow}$, it belongs to the WJ sample. The final HJ and WJ sample includes 216 Kepler giant planets. Figure 4(C) shows the distribution of the orbital period of planets and the mass of their host stars.

The survey completeness of a planet with given period P and radius R_p is obtained by a Kepler Survey Simulator[44]. Then, we divide 216 planets into five bins according to the effective temperature T_{eff} of their host stars. Since most samples concentrate between $5000K$ and $6000K$, we use a non-uniform bin size to contain enough samples within the boundary bins. The bin size is 500K for the three bins in the middle, and we set all samples with $T_{eff} < 4600K$ to the left boundary bin and all samples with $T_{eff} > 6100K$ to the right boundary bin (Figure 4 (B)). The color map shows the survey completeness of each planet where brighter color denotes higher completeness.

Furthermore, we also build WJ and CJ use RV-detected giant planet.If equilibrium temperature of RV-detected giant planet is less than 170K, which means it is outside the snow line, $a_p > a_{snow}$, then we set this planet into to the CJ sample. Similarly, if its equilibrium temperature is higher than 170K and then it belongs to the WJ sample. Note that, the RV-detected and Kepler samples are analyzed separately in this study.

RV Samples

To get sufficient long period giant planets, we use RV-detected planets to build our CJ and WJ sample. And to avoid systemic differences in planetary and stellar properties imposed by various fitting models adopted by different surveys and obtain reliable survey completeness, we select our RV samples only based on the HARPS and CORALIE survey[27,33]. There is a total of 1797 stars with K, G and F stellar type, of which 131 host planets. We then cross match them with the Gaia DR2 database[45] to get high precision stellar properties, such as radius, luminosity and T_{eff}. Only stars with T_{eff} between 4600K and 6600K are selected for further analysis to avoid systematic errors caused by the known limitation of synthetic stellar atmospheric models[46]. Our final RV-related sample for calculating planetary occurrence rates and stellar property dependencies contains 1191 stars. And there are several more criteria have been applied to filter planetary sample:

1. We only choose those confirmed RV-detected giant planets with $0.3M_J < M_p < 13M_J$(M_J is mass of Jupiter).

2. Giant planets with orbital semi-major axis less than $0.1a_{snow}$(a_{snow} is the location of snow line) are excluded. For RV samples, the sample only include CJ and WJ.

3. Giant planet with orbital period larger than 15000 days are excluded.The reason is that the survey completeness obtained by the HARPS and CORALIE survey is only valid for planets with period shorter than 15000 days[27].

The final RV-related sample includes 1191 stars, of which 85 stars hosting 99 RV-detected giant planets. Figure 4 (C) shows the distribution of the orbital period of planets and the mass of their host.

We extract survey completeness for each RV-detected planet from the study of HARPS and CORALIE survey[27]. Each curve in the Figure 6 of the paper[27] represents the fraction of stars with sufficient measurements to detect a planet at a given period P and minimum mass $Msini$. We linearly interpolate these curves into a uniform grid with $Msini$ between 0.3 and 13 M_J and period between 1 and 15000 days. The survey completeness of every selected RV-detected planet is extracted by averaging the grid where it falls. The total sample is then divided into several bins according to the T_{eff} of their hosts in the range of $4600-6600K$, where the binning size is 500K. Color map in Figure 4(A) shows the interpolated survey completeness of every giant planet in a $Msini$-T_{eff} plane.

Occurrence Rates

In this study, we are trying to reveal the orbital evolution history of different kind of giant plants through investigating the correlations between their occurrence rates and their host's stellar properties. There are two reasons for why we select the effective temperature as a major representative host property. First, the effective temperature is highly related to the stellar mass, spectral type and even properties of the proto-stellar disk. Second, the measurement on effective temperature is usually easier to achieve higher accuracy. The effective temperature of the RV-detected(Kepler) samples ranges from $4600K$($3600K$) to $6600K$ ($7100K$). As mention in last section, we first divide this range into several bins. Then, to get the occurrence rate of a kind of giant planets orbiting their host stars in a single effective temperature bin. For RV-detected samples, the procedure of calculate the occurrence rates of giant planets in the specific effective temperature bin is as follows:

1. According to the effective temperature of the whole star sample in the specific RV survey(here, we focus on HARPS & CORALIE survey) to get the number $N^*_\star$ of star in the specific effective temperature bins. The number of stars corresponds to four T_{eff} bins are listed in table 1.

2. For every RV-detected giant planets that around the star in the specific effective temperature bins, to get the survey completeness $p^*{}_j$ on the basis of minimum mass and period of the giant planets(shows as color of point in 4(A)) .

3. To calculate the occurrence rate, i.e.,the average number of giant planets per one star in the specific effective temperature bin:

$$\eta_{RV} = \frac{1}{N^*_\star}\sum_{j=1}^{n^*_p}\frac{1}{p^*{}_j} \tag{3}$$

where $n^*{}_p$ is the detected number of planets per effective temperature bin in RV survey(shown in table 1).

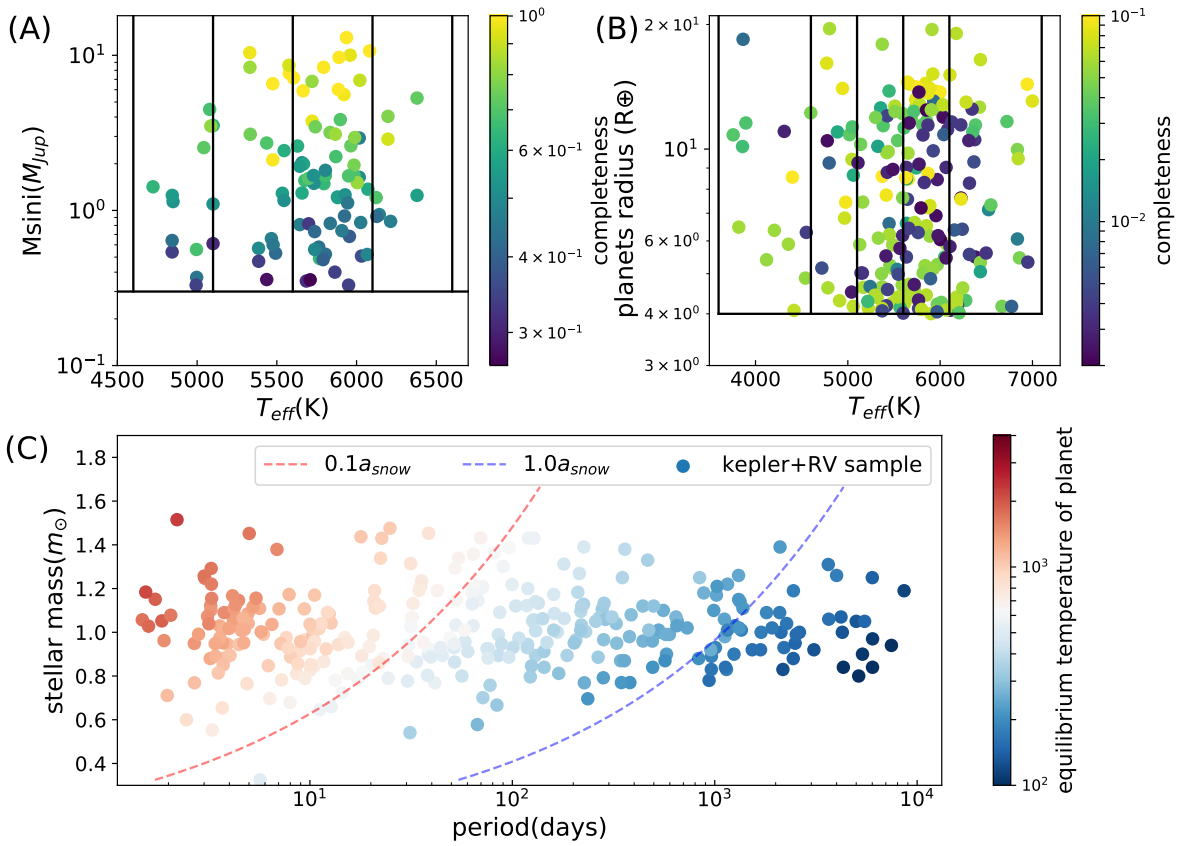

Figure 4. Overview of our samples.(A): distribution of planetary mass and effective temperature of host star(m_p-T_{eff}) of RV giant planets samples, detection completeness shown as color contours from 0.0 to 1.0 in steps of 0.1 (B): distribution of planetary radius and effective temperature of host star (R_p-T_{eff}) of Kepler giant planets samples, detection completeness shown as color contours; (C): the period-stellar mass distribution of orbital period and stellar mass(p-T_{eff}) of all samples, the colors denote the equilibrium temperature of each giant planets, where red dotted line and blue line are mark the position of 0.1a_{snow} and 1.0a_{snow} of different host stars.

Table 1. Number of stars and giant planet in RV -detected samples

Effective Temperature(K)	Number of stars($N^*_\star$)	Number of giant planets(n^*_p)
(4600, 5100]	244	12
(5100, 5600]	334	18
(5600, 6100]	508	61
(6100, 7100]	105	8

Table 2. Number of stars and giant planet in Kepler samples

Effective Temperature(K)	Number of stars($N_\star$)	Number of giant planets(n_p)
(3600, 4600]	8052	14
(4600, 5100]	10904	17
(5100, 5600]	26539	52
(5600, 6100]	41243	88
(6100, 7100]	24650	45

For transiting giant planets, the process of calculating the occurrence rate of giant planets in a single effective temperature bin is describe below:

1. To obtain statistics $N_\star$ of star in each effective temperature bins. Note that $N_\star$ for different bin not only the star hold giant planets, but all of specific stars found in the target sky area of the Transit survey. Table 2 describe the number of stars per effective temperature bin in Kepler survey.

2. According to the observational pipeline of the Transit survey, to obtain detection efficiency f_{det} of every giant planet. The color of circle in Figures 4 (B) shows the detection efficiency f_{det} of each transit samples.

3. we calculate the geometric transit probability of a transiting giant planets. When planets' radius is R_p, it orbits its primary(radius of host is $R_\star$) with orbital semi-major axis a and orbital eccentricity e, the geometric transit probability f_{geo} is :

$$f_{geo} = \frac{R_\star + R_p}{a(1-e^2)} \tag{4}$$

   Where $R_\star$ is the correctional value after the Gaia-Kepler cross-match, and R_p is calculated by the new $R_\star$ and the ratio of planet to stellar radius.

4. To obtain the survey completeness p_j evaluate of a transiting orientation of each planet j, which combine the detection efficiency $f_{det,j}$and the geometric transit probability$f_{det,j}$ of each giant planet:

$$p_j = f_{det,j} \times f_{geo,j} \tag{5}$$

5. To obtain the occurrence rate, i.e.,the average number of giant planets per one star in the specific effective temperature bin:

$$\eta_{Kepler} = \frac{1}{N_\star} \sum_{j=1}^{n_p} \frac{1}{p_j} \tag{6}$$

   where n_p is the detected number of planets per effective temperature bin in Kepler survey(listed in table 2).

The uncertainty on the occurrence rate is calculated from the square root of the number of detected planets per bin.

Consistency check: Definition of HJ, WJ and CJ use the period

Giant planets with orbital period less than 10 days are usually called hot Jupiter, those with moderate orbital period (from 10 days to 200days) are called warm Jupiter , and those with long orbital period ($>$ 200 days) are called cold Jupiter. Such definitions based on a fact that the equilibrium temperature of planet depends on its distance to the host star. But for planetary systems with different type of stars, stellar properties may also play a crucial role to determine a planet is hot or cold. That's the

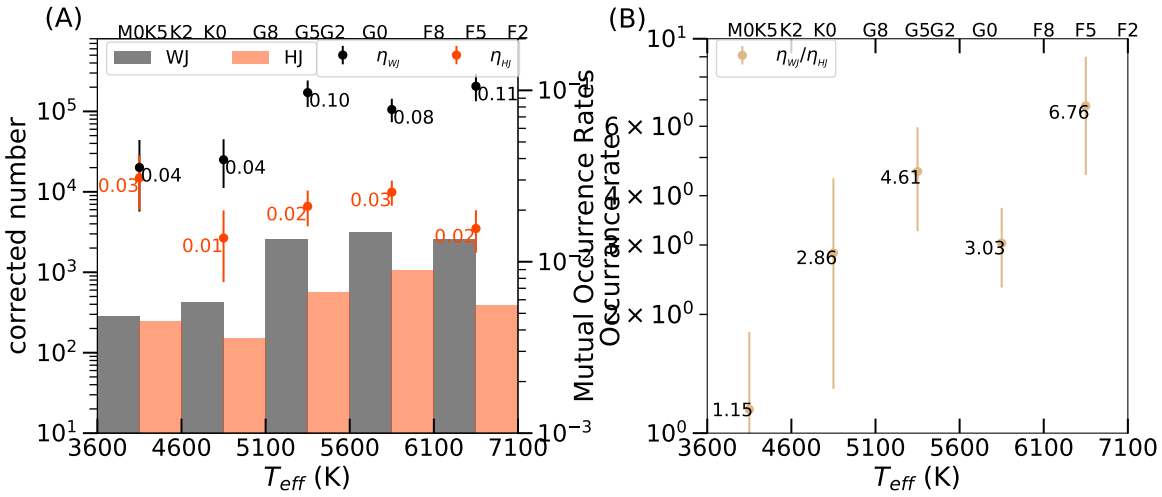

Figure 5. Similar to Figure 1(c)and (D), but here, HJ(orange),WJ(gray) and CJ(blue) are defined only depends on planetary orbit period.

reason we propose a new definition to distinguish HJ, WJ and CJ. However, the previous definitions have been used for a while, it is reasonable for us to compare the occurrence rates with different definitions and find out its influences to our final results.

For RV-detected samples, because the small number of WJ(2,4,5,1 giant planets in each T_{eff} bins). So, using the traditional definition of WJ and CJ in RV-detected samples, we can't obtain some information about the occurrence rates of WJ, and lead to misunderstand the ratio of their occurrence rates (η_{CJ}/η_{WJ}). However, the kepler sample maybe provide more WJ sample to further analysis the occurrence rates of WJ in period- boundary definition.

We calculate the occurrence rates of WJ and HJ, whose definition only depends on planetary orbit period, in the Kepler sample. Figure 5(A), the occurrence rates of WJ and HJ are both increasing with host effective temperature when $T_{eff} \leq 6100K$ and drop down a bit when T_{eff} is higher. For all the M/K/G/F stars, WJ has a higher probability to exist than HJ. The ratio of their occurrence rates (η_{WJ}/η_{HJ}) is always above 1 and has an increasing trend with the increasing stellar effective temperature (see in Figure 5(B)). This result is quite similar to that when new definition is adopted. There are two major differences: First, in the rightmost temperature bin where $T_{eff} \in (6100K, 7100K]$, with our new definition, the number of WJ (after survey completeness correction) drops more than that of traditional WJ does. In contrast, the number of new-defined HJ keeps increasing within the same temperature bin, where the number of traditional HJ decreases. Second, with our new definition, the ratio of occurrence rates (WJ to HJ) is higher than the corresponding value derived from traditional definition in each T_{eff} bin. It is clearly that some traditional WJ which is classified purely by their orbital period are actually quite hot because of the high temperature of their host. And such mis-classification effect is more obvious when the host is of higher effective temperature, e.g. those F or earlier type stars. For late type stars, e.g. M, K and G stars, the two occurrence-rate-effective-temperature trends are consistent, which means there are indeed some physics mechanisms behind.

Consistency check: The hypothesis of In-situ formation

We first assume the formation efficiency of giant planet is position-independent, which means the probability where a giant planet may show up is uniform within a planetary system. This is obviously not true, but could be used as a reference. In this case, giant planets distribute uniformly in space and the odd of a giant planet becomes WJ or CJ depends only on the position of the snow line. In other words, the ratio of formation rate η'_{CJ}/η'_{WJ} is the ratio of the distance from the snow line to the outer boundary of the system to the distance from the host to the snow line. Since our definitions on HJ, WJ and CJ depend on the position of snow line, $a_p \leq 0.1a_{snow}$, $0.1a_{snow} < a_p \leq 1.0a_{snow}$ and $a_p > 1.0a_{snow}$, respectively, we set the outer boundary to $5a_{snow}$. Then, as the place of snow line, a_{snow}, moving outward with increasing stellar effective temperature, the outer boundary also increases. As a result, the ratio η'_{CJ}/η'_{WJ} is constant and does not change with stellar type in this case (See the upper horizontal solid orange line in Figure 6).

Then we further assume the efficiency to form a giant planet is position-dependent, which means the probability where a giant planet may show up depends on the surface density and dust collision timescale——the higher surface density and shorter collision timescale are, the easier for a place to form a giant planet. We assume the formation rates is proportional to the potential mass of planetary building blocks inside and outside the snow-line, M_{CJ} and M_{WJ}. Therefore, the ratio of the

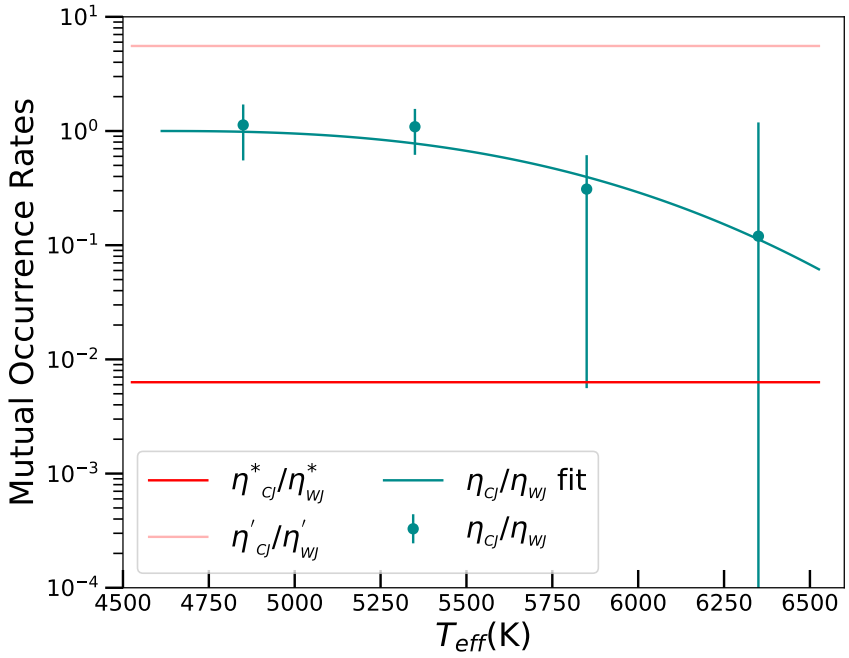

Figure 6. The comparison of the simulation and the observational result of mutual occurrence-rate-T_{eff} dependence of CJ and WJ. The green curve is the best fit of result(1(b)). The pink curve and the red curve show the simulation result of ratio of occurrence rate based on position-independent and position-dependent hypothesis, respectively.

formation rate, ${\eta^*}_{CJ}/{\eta^*}_{WJ}$, could be represented by the mass ratio, M_{CJ}/M_{WJ}:

$$ {\eta^*}_{CJ}/{\eta^*}_{WJ} = M_{CJ}/M_{WJ} \tag{7} $$

where mass of all planetary building blocks M_{CJ} and M_{WJ} are determined by the a function of solid and gaseous mass density and solid accretion timescale, which reads as follow:

$$ M_{WJ} = \int_{0.1a_{snow}}^{1.0a_{snow}} \frac{2\pi x(\Sigma_g(x)+\Sigma_d(x))}{t_{acc}} \mathrm{d}x \tag{8} $$

$$ M_{CJ} = \int_{1.0a_{snow}}^{5.0a_{snow}} \frac{2\pi x(\Sigma_g(x)+\Sigma_d(x))}{t_{acc}} \mathrm{d}x \tag{9} $$

which t_{acc} is the solid cores' accretion timescale[47]:

$$ t_{acc} \sim {\Sigma_d}^{-1}{\Sigma_g}^{-2/5}{M_*}^{-1/6} yr \tag{10} $$

Σ_d and Σ_g is the surface density of dust and gas within the protoplanetary disk:

$$ \Sigma_d = f_d f_{snow} \times 10(\frac{a_p}{1AU})^{-3/2} gcm^{-2} \tag{11} $$

$$ \Sigma_g = f_g(2.4\times10^3)(\frac{a_p}{1AU})^{-3/2} gcm^{-2} \tag{12} $$

We adopt the host star dependence f_d, f_g and f_{snow}: $f_d = 0.7{M_*}^{1.9}$, $f_{snow} = 1$(inside snow line), $f_{snow} = 4.2$(outside snow-line) , and we adopt $f_d = f_g$ that represent the solar abundance. We calculate the ratio ${\eta^*}_{CJ}/{\eta^*}_{WJ}$ around stars with different

effective temperatures and the result is shown by the lower horizontal solid blue line in Figure 6. Because of the stellar effective temperatures is concerned only with mass of host, and the stellar mass is eliminate in the calculation of the ratio η^*_{CJ}/η^*_{WJ}, so it is also a constant even though the stellar effective temperatures is change. It is clearly that both two cases assuming in-situ formation are significantly different from the observation result. Sothe in-situ mechanism can not explain our result.

LEAD CONTACT WEBSITE

Ji-Lin Zhou: https://orcid.org/0000-0003-1680-2940; Hui Zhang: https://orcid.org/0000-0003-3491-6394; Xiang-Ning Su: https://orcid.org/0000-0003-3624-6881.